Ab Initio Density Functional Calculations of Deuterium Kinetic Isotope Effects for Decomposition of Dimethylnitramine

Nathan J. Harris* and Koop Lammertsma*

Department of Chemistry, University of Alabama at Birmingham, Birmingham, Alabama 35294, and Department of Chemistry, Vrije Universiteit, 1081 HV Amsterdam, The Netherlands

Received: July 31, 1996; In Final Form: November 8, 1996[⊗]

Ab initio harmonic force fields were computed using the Becke3−Lee−Yang−Parr hybrid density functional with the standard 6-31G* basis set for dimethylnitramine, for dimethylamino radical, and for the transition structure for five-center elimination of HONO from dimethylnitramine. These force fields were used to calculate the primary deuterium kinetic isotope effect for the HONO elimination, and the secondary isotope effect for the N−N bond homolysis of dimethylnitramine. The computed primary effect is $k^H/k^{D6} = 4.21$, and the computed secondary effect is $k^H/k^{D6} = 1.40$, both at 240 °C. Comparison with the experimentally observed isotope effect of 1.57 for decomposition of dimethylnitramine-d_6 in solution at 240 °C suggests a significant part of the observed effect is due to the secondary effect on N−N bond homolysis. Similar β secondary deuterium isotope effects are expected for the N−NO_2 cleavages that initiate the decompositions of the nitramine explosives HMX and RDX.

Introduction

The decomposition of dimethylnitramine (DMNA) has been studied as a model for decomposition of more complex nitramine explosives such as hexahydro-1,3,5-trinitro-*s*-triazine (RDX) and octahydro-1,3,5,7-tretranitro-1,3,5,7-tetrazocine (HMX).[1] McQuaid identified three possible unimolecular pathways[2] for DMNA decomposition: (1) simple N−N homolysis, (2) rearrangement to a nitrite ester, Me_2NONO, and (3) concerted elimination of nitrous acid, HONO, through a five-center transition structure.

$$Me_2NNO_2 \rightarrow Me_2N + NO_2 \qquad (R1)$$

$$Me_2NNO_2 \rightarrow Me_2NONO \qquad (R2)$$

$$Me_2NNO_2 \rightarrow [TS] \rightarrow CH_2NMe + NO_2H \qquad (R3)$$

The N−N bond homolysis is the predominant pathway in the gas phase decomposition of DMNA using infrared multiphoton decomposition (IRMPD).[1,3] The N−N homolysis also is the main pathway in the solution phase decomposition at 200−300 °C.[4] Botcher and Wight[5] found N−NO_2 homolysis was the initial reaction in the laser pyrolysis of solid RDX. Rearrangement to the nitrite was reported in one instance,[3b,6] when DMNA was decomposed by IRMPD under collisional conditions. In IRMPD of nitromethane the C−N homolysis and rearrangement to nitrite are competitive pathways.[6b,7] The third pathway, concerted HONO elimination, has not been observed directly for DMNA. Oxley suggested the elimination competes with N−N cleavage in solution.[4] This conclusion was based on observation of a deuterium kinetic isotope effect (KIE) of $k^H/k^{D6} = 1.57$ at 240 °C. Primary KIEs are also observed in the condensed phase decompositions of RDX and HMX.[8] Shaw and Walker speculated that HONO elimination could be a minor pathway in unimolecular decomposition of HMX.[9] Also, Capellos[10a] and Zuckermann[10b] have suggested RDX reacts by HONO elimination in the gas phase. The elimination certainly takes place in the hydrocarbon analogue 2-nitropropane, and the kinetic barrier for this process was determined by Benson[11] and later by Wodtke et. al.[7]

In the present work, we study the competing N−N cleavage and HONO elimination pathways using ab initio MO theory. Theoretical deuterium kinetic isotope effects are computed for these two pathways. Interestingly, we find the N−N bond cleavage has a significant secondary KIE for β deuterium substitution that arises from hyperconjugation of the amino radical with the adjacent C−H bonds. Although previous explanations[4,8] focus on a primary KIE for rate-determining C−H bond cleavage, we suggest the secondary effect on N−N bond cleavage contributes significantly to the KIE in unimolecular dimethylnitramine decomposition.

Methods

Ab initio calculations were carried out using the Gaussian 94 programs.[12] Energies, geometries, and harmonic vibrational frequencies were computed using the Becke3−Lee−Yang−Parr (B3LYP) hybrid density functional[13] with the standard 6-31G* basis set.[14,15a] Computations were carried out on dimethylnitramine (DMNA), dimethylamino radical (Me_2N), NO_2 radical, the transition structure (TS) for elimination of HONO from DMNA, nitrous acid (HONO), and *N*-methylmethylenimine ($MeNCH_2$). Geometries for DMNA and TS are described in Tables 1 and 2. Absolute energies and zero-point vibrational energies for all structures are given in Table 3. B3LYP harmonic frequencies were computed as well for the perdeuterated analogues DMNA-d_6, Me_2N-d_6, and TS-d_6. The same calculations were also done using second-order Moller−Plesset theory,[15a] with the frozen core approximation, again using the 6-31G* basis set (i.e., MP2(fc)/6-31G*).[15b]

The harmonic frequencies for the isotopic pairs (DMNA/DMNA-d_6), (TS/TS-d_6), and (Me_2N/Me_2N-d_6) were used to compute the KIE for the concerted elimination of HONO and for the N−N bond homolysis.[16,17] A FORTRAN program for computing isotope effects from frequencies is included in the Supporting Information, along with a table of harmonic frequencies for TS and TS-d_6.

Briefly, the reduced isotopic partition function ratios[16a,c] $(s_2/s_1)f$ were computed using the computed harmonic frequencies

[⊗] Abstract published in *Advance ACS Abstracts,* January 1, 1997.

S1089-5639(96)02326-2 CCC: $14.00

TABLE 1: B3LYP/6-31G* Geometries for DMNA (See Figure 1) Compared with Experimental Geometries from Ref 19 (Bond Lengths, angstroms; Angles, degrees)

		expt				expt	
	B3LYP	*a*	*b*		B3LYP	*a*	*b*
N−N	1.384	1.331(3)	1.383(3)	C−N−C	120.3	124.6(2)	127.6(6)
N−C	1.458	1.452(3)	1.460(3)	C−N−N	115.5	117.7(2)	116.2(3)
N−O	1.232	1.240(2)	1.223(2)	C−N−O	126.0	124.0(2)	130.4(3)
				O−O−N	117.0	118.0(2)	114.8(2)
				γ^c	30.3	0.00	0.00

[a] X-ray crystal structure from ref 19a. [b] Gas phase geometry from electron diffraction.[19b] [c] γ is the pyramidalization of the amine nitrogen, expressed as the angle between the CNC plane and the NN bond axis.

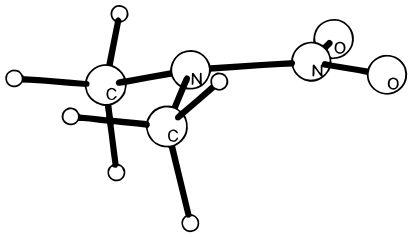

Figure 1. B3LYP/6-31G* geometry for dimethylnitramine (DMNA).

TABLE 2: B3LYP/6-31G* Geometries for TS (See Figure 2 for Numbering of Atoms) (Bond Lengths, angstroms; Bond Angles, degrees)

N1−N2	2.190	N2−O2	1.206
N1−C1	1.343	O1−H1	1.320
N1−C2	1.451	H1−C1	1.314
N2−O1	1.270		
C−N1−C	117.1	N1−N2−O1	101.6
C1−N1−N2	94.6	N1−N2−O2	135.9
C2−N1−N2	97.2	H1−C1−N1	97.0
O−N2−O	122.2	H2−C1−N1	115.0
O1−H1−C1	152.3	H3−C1−N1	119.7
C1−N1−N2−O1	6.5	C1−N1−N2−O2	180.1
γ^a		29.6	

[a] γ is pyramidalization of C1, expressed as the angle between the H2C1H3 plane and the C1N1 bond axis.

TABLE 3: Absolute B3LYP/6-31G* energies (hartrees, 1 hartree = 627.51 kcal/mol), and Zero-Point Vibrational Energies (ZPVE; kcal/mol)

	energy	ZPE		energy	ZPE
DMNA	−339.656 546	60.08	HONO	−205.696 797	12.75
TS	−339.576 607	55.12	$MeNCH_2$	−133.942 339	43.04
Me_2N	−134.509 485	48.66	NO_2	−205.072 205	5.54

for DMNA/DMNA-d_6, TS/TS-d_6, and Me_2N/Me_2N-d_6. The KIE for the N−N dissociation reaction (eq R1) was computed from the ratio $(s_2/s_1)f_{DMNA}/(s_2/s_1)f_{Me_2N}$. Similarly, the KIE for the HONO elimination (eq R2) was computed from KIE = $(Q_t^H/Q_t^D)(s_2/s_1)f_{DMNA}/(s_2/s_1)f_{TS}$.[17] The factor (Q_t^H/Q_t^D) is a tunneling correction calculated with Bell's equation.[17b,18]

The tunneling correction factor is given by $Q_t^H/Q_t^D = (|u^H/2|/\sin|u^H/2|)/(|u^D/2|/\sin|u^D/2|)$, where $|u| = h|\nu^*|/kT$, and ν^* is the imaginary frequency in the transition structure.[18] This correction is valid if $|u| < 2\pi$ and if the potential energy is a quadratic function of the reaction coordinate in the region of the saddle point.

Results and Discussion

Geometries and Energies. The theoretical geometry for dimethylnitramine is compared with the experimental gas phase and solid phase geometries[19] in Table 1. Both experimental geometries are planar ($\gamma = 0.00°$), with C_{2v} symmetry, while the B3LYP/6-31G* structure (Figure 1) is pyramidal at the amine nitrogen ($\gamma = 30.3°$; see Table 1), with C_s symmetry.

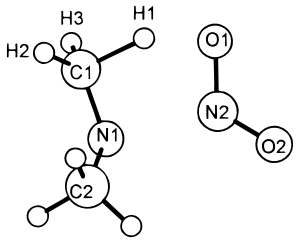

Figure 2. B3LYP/6-31G* geometry for the transition structure (TS) for elimination of HONO from dimethylnitramine

The MP2/6-31G* and B3LYP/6-31G* geometries are very similar, except the amine is more pyramidal ($\gamma = 38.5°$) and the N−O bonds are 0.009 Å longer in the MP2 geometry.

Compared with the theoretical structure, the experimental X-ray crystal structure[19a] has a short N−N bond, long N−O bonds, and a wide C−N−C angle (Table 1). These differences, and the planar geometry in the solid, suggest that electron donation from the amine lone pair to the nitro group is more important in the solid than in the gas phase.[20] This might be caused by intermolecular electrostatic interactions which lead to enhanced resonance in the crystalline state.

The experimental gas phase structure for DMNA[19b] also differs considerably from the theoretical gas phase geometry. The large differences in the C−N−C and O−N−O angles and in the pyramidalization of the amine[20] suggest the experimental gas phase geometry is inaccurate.

In the transition structure for HONO elimination (see Figure 2 and Table 2) the breaking CH bond and the forming OH bond have nearly equal lengths. The N−N bond in TS is stretched to 2.19 Å, and the nitro group and N1, C1, and H1 atoms form a nearly planar five-membered ring. The C−H−O angle around the transfered hydrogen is nonlinear at 152.3°. In the MP2/6-31G* transition structure the breaking C−H bond is longer by 0.024 Å, the forming O−H bond is shorter by 0.028 Å, and the breaking N−N bond is shorter by 0.150 Å than in the B3LYP/6-31G* structure.

The B3LYP/6-31G* harmonic frequencies for DMNA and DMNA-d_6 are given in Table 4a, and the observed infrared frequencies for DMNA[3a] are given in Table 4b. The most intense bands in the theoretical spectrum are assigned to the NO_2 symmetric and assymetric stretching modes at 1355 and 1652 cm^{-1}, respectively. These are in good agreement with the observed bands at 1300 and 1560 cm^{-1}, after allowance is made for vibrational anharmonicity, which tends to make the observed frequencies about 5% smaller than the theoretical harmonic frequencies.[16c]

The B3LYP/6-31G* enthalpy barrier at 0 K for the N−N cleavage is 41.08 kcal/mol (Table 5). At PMP2/6-31G* the bond enthalpy increases to 45.11 kcal/mol. Some experimental estimates for the N−N bond dissociation enthalpy for DMNA at 298 K are 45.9,[21] 46.5,[3b] and 46.2 kcal/mol.[9] These are smaller than the C−N bond dissociation enthalpy of 53 kcal/mol for the carbon analogue 2-nitropropane.[7]

TABLE 4

(a) B3LYP/6-31g* Harmonic Vibrational Frequencies for Dimethylnitramine and Dimethylnitramine-d_6 (IR intensities (kM/mol) in parentheses)

ν^H (cm^{-1})	ν^D (cm^{-1})	assignment
118 (0.1)	91	a″ NN torsion + CN torsion
123 (3)	92	a′ CN torsion
137 (0.3)	121	a″ CN torsion
205 (9)	185	a′ amine inversion
358 (2)	324	a″ CNN bend
421 (4)	360	a′ CNC bend
615 (10)	588	a″ skeletal def
623 (1)	589	a′ skeletal def
778 (20)	774	a′ NO_2 out of plane def
859 (10)	799	a′ ONO bend + CN str
1011 (68)	835	a′ HCN bend + NN str + CN str
1064 (13)	867	a″ HCN bend
1138 (3)	895	a″ HCN bend
1165 (50)	927	a′ HCN bend
1284 (4)	1080	a′ NN str + HCN bend + CNC bend
1325 (2)	1089	a″ CN str + HCN bend
1355 (278)	1092	a′ NO_2 sym str + N−N str + HCH bend
1457 (6)	1101	a″ HCH bend
1497 (35)	1108	a′ HCH bend
1504 (12)	1138	a″ HCH bend
1522 (11)	1198	a′ HCH bend
1524 (1)	1300	a″ HCH bend
1543 (38)	1376	a′ HCH bend
1652 (265)	1649	a″ NO_2 assym str
3041 (23)	2189	a″ CH str
3046 (44)	2195	a′ CH str
3136 (0.1)	2319	a″ CH str
3142 (33)	2321	a′ CH str
3190 (2)	2365	a″ CH str
3192 (5)	2369	a′ CH str

(b) Experimental Fundamental Frequencies (cm^{-1}) for Dimethylnitramine from Ref 3a (Degeneracies in Parentheses)

2940 (6)	C−H str	1150 (6)	H−C−N bend
1560	N−O str	1100 (2)	C−N str
1430 (4)	H−C−H bend	800 (2)	C−N−N bend
1300	N−O str	640 (3)	N−N−O bend
1250	N−N str	230 (2)	C−N torsion
1200	C−N−C bend	150	N−N torsion

TABLE 5: B3LYP/6-31G* Energies in kcal/mol, Corrected for ZVPE

DMNA → $Me_2N + NO_2$	ΔE = 41.08 kcal/mol
DMNA → [TS]	ΔE = 45.20 kcal/mol
DMNA → $MeNCH_2$ + HONO	ΔE = 6.64 kcal/mol

The bond dissociation enthalpy at 0 K for the parent nitramine, NH_2NO_2, is 51.1 kcal/mol using the accurate G2 theory,[22] compared to 47.0 kcal/mol computed with B3LYP/6-31G*. This suggests the B3LYP/6-31G* enthalpy for N−N cleavage in DMNA should be adjusted upward to 45.2 kcal/mol, which increases to 47 kcal/mol after a temperature correction to 298 K. This gives better agreement with the experimental data.

The HONO elimination has never been observed directly for DMNA or other nitramines. The B3LYP/6-31G* enthalpy barrier at 0 K is 45.20 kcal/mol (Table 5). At MP2/6-31G* this increases to 53.83 kcal/mol. Lazarou[3a] suggests the barrier should be the same as the 41−43 kcal/mol barrier for HONO elimination in 2-nitropropane,[7] but Melius[21] suggests the barrier for the nitramine should be 2 kcal/mol lower than for the carbon analogue. The computed enthalpy change for formation of HONO + $MeNCH_2$ is 6.64 kcal/mol at 0 K, compared with other estimates of −1 [9] and +3 kcal/mol [3a] for the enthalpy change at 298 K.

It appears that our B3LYP/6-31G* barrier for N−N cleavage is underestimated by 5 kcal/mol and our barrier for HONO elimination is overestimated by 2−6 kcal/mol. The MP2/6-31G* theory also incorrectly indicates the HONO elimination barrier to be higher in energy than the barrier for N−N cleavage. We suspect that a multireference configuration interaction approach would be better than B3LYP or MP2 for computing the energy difference between the two competing pathways,[23,6] but such calculations are presently beyond our means.

TABLE 6: Computed Isotope Effects at 240 °C

DMNA → $Me_2N + NO_2$	k^H/k^{D6} = 1.40 (1.37[a])
DMNA → [TS] → CH_2NMe + HONO	k^H/k^{D6} = 4.21 (4.02[a])

[a] Computed using 0.95 scaled B3LYP/6-31G* frequencies.

The HONO elimination pathway is entropically more demanding than the N−N cleavage. This is reflected in the difference in preexponential Arrhenius factors—log A = 12 for HONO elimination and log A = 15.5 for N−N cleavage.[3a,7,11]

Uncertainty in the Arrhenius parameters, especially in the activation barrier for the HONO elimination, makes it difficult to estimate the branching ratio for the two pathways, but it has been suggested that the elimination is a minor pathway if it is present at all.[3c,4,9]

The branching ratio is given by the Arrhenius expression $k_1/k_2 = (A_1/A_2)\exp(-\Delta E_a/RT)$. Both the preexponential factor and the activation energy are larger for the N−N cleavage pathway (k_1) than for the elimination pathway (k_2). We can estimate the difference ΔE_a = 4 kcal/mol in activation barriers and the difference $\Delta\log A$ = 3 in preexponential factors. This gives a branching ratio of k_1/k_2 = 14 at 200 °C and k_1/k_2 = 30 at 300 °C in favor of N−N cleavage. However, small uncertainties of 0.5 in $\Delta\log A$ and 1 kcal/mol in ΔE_a lead to a factor of 9 uncertainty in the branching ratio.

Kinetic Isotope Effects. The computed KIEs for the N−N bond cleavage and HONO elimination are presented in Table 6. The computed primary KIE for HONO elimination is 4.21 at 240 °C, which includes a correction factor of 1.41 for quantum tunneling. The MP2/6-31G* primary KIE is 4.42, including tunneling. Superimposed on the primary KIE for the HONO elimination is a secondary KIE for the remaining hydrogens (or deuteriums) which are not transferred.

The true primary KIE can be computed from the vibrational frequencies of the monodeuterated DMNA-d_1 and TS-d_1 as k^H/k^{D1} = 3.36, including a correction factor of 1.39 for tunneling. The remaining KIE of 4.21/3.36 = 1.25 represents the superimposed secondary KIE due to the five hydrogens or deuteriums that are not transferred.

The B3LYP/6-31G* β secondary KIE for N−N cleavage (Table 6) is 1.40 at 240 °C. The MP2/6-31G* secondary KIE is 1.29. This is a significant effect compared with the observed KIE of 1.57 in solution at 240 °C.[4]

Observed fundamental frequencies tend to be about 5% smaller than harmonic frequencies, due to anharmonicity.[16c] The simplest method for correcting for anharmonic effects is to uniformly scale the theoretical harmonic frequencies. The primary KIE computed using a scaling factor of 0.95 is 4.02 (including tunneling), and the secondary KIE is 1.37. As expected, uniform scaling of frequencies has little impact on the computed isotope effects.[16c]

The secondary KIE is caused by hyperconjugation of the nitrogen radical with the six adjacent C−H or C−D bonds. The resulting weakening of these bonds causes fractionation[24] of the lighter isotope in the amino radical. A similar effect causes a decrease in the gas phase acidity of CD_3OH relative to CH_3OH.[25] Conjugation with the oxyanion leads to weakening of the adjacent C−H or C−D bonds in the isotopic methoxides.[25]

Using Oxley's observed KIE[4] of $(k^H/k^{D6})_{obs}$ = 1.57 and our calculated KIEs of $(k_1{}^H/k_1{}^{D6})$ = 1.40 and $(k_2{}^H/k_2{}^{D6})$ = 4.21 for the two pathways, we can compute the branching ratios $k_1{}^H/$

$k_2^H = 5.2$ and $k_1^{D6}/k_2^{D6} = 15$.[26a] These are the ratios of N−N cleavage (k_1) to HONO elimination (k_2) for the protio and deuterio species at 240 °C. The branching ratio favors the N−N cleavage over the HONO elimination, as expected. Deuterium substitution increases the preference for the N−N cleavage pathway.

Small errors in the observed KIE or the calculated secondary KIE would change the estimated branching ratio considerably.[26b] A further source of ambiguity is that other minor reaction pathways besides the HONO elimination might exist. Certainly the condensed phase decompositions of RDX and HMX are complex and involve several parallel reaction pathways.[27]

The observed isotope effects for decomposition of RDX-d_6 and HMX-d_8 have been interpreted as primary effects operating on decomposition pathways involving rate-determining C−H (or C−D) bond breaking.[8] These isotope effects, measured by isothermal differential scanning calorimetry,[8] are isotope effects on the *global* rates for release of energy from HMX or RDX. These global rates are not related in a simple way to the rate for an initiating chemical reaction such as $N-NO_2$ cleavage. Although the β secondary isotope effect for $N-NO_2$ cleavage in DMNA also acts on the $N-NO_2$ cleavages in the nitramine explosives, this effect is unlikely to contribute to the overall isotope effect on the global decomposition rate.

Conclusion

Our theoretical results suggest that significant part of the overall deuterium isotope effect for unimolecular dimethylnitramine decomposition is a β secondary effect operating on the $N-NO_2$ bond homolysis. The same secondary effect should act on the initiation of decomposition of the nitramine explosives HMX and RDX. However, the experimentally observed isotope effects on the global decomposition rates of HMX and RDX in the condensed phase are best interpreted as primary effects operating on pathways that involve rate-determining C−H (or C−D) homolysis.

Acknowledgment. This work was supported by the U. S. Air Force Office of Scientific Research under Grant F49620-94-1-0451.

Supporting Information Available: A table listing B3LYP/6-31G* harmonic frequencies for TS and TS-d_6 and text giving a 130 line FORTRAN program for computing the reduced isotopic partition function ratio (s_2/s_1)f for two isotopomers (8 pages). Ordering information is given on any current masthead page.

References and Notes

(1) Adams, G. F.; Shaw, R. W., Jr. *Annu. Rev. Phys. Chem.* **1992**, *43*, 311−340.

(2) McQuaid, M. J.; Miziolek, A. W.; Sausa, R. C.; Merrow, C. N. *J. Phys. Chem.* **1991**, *95*, 2713−2718.

(3) (a) Lazarou, Y. G.; Papagiannakopoulos, P. *J. Phys. Chem.* **1990**, *94*, 7114−7119. (b) Stewart, P. H.; Jeffries, J. B.; Zellweger, J. M.; McMillan, D. F. *J. Phys. Chem.* **1989**, *93*, 3557−3563. (c) Sumpter, B. G.; Thompson, D. L. *J. Chem. Phys.* **1988**, *88*, 6889−6897.

(4) Oxley, J. C.; Hiskey, M.; Naud, D.; Szekeres, R. *J. Phys. Chem.* **1992**, *96*, 2505−2509. Oxley, J. C.; Kooh, A. B.; Szekeres, R.; Zheng, W. *J. Phys. Chem.* **1994**, *98*, 7004−7008.

(5) Botcher, T. R.; Wight, C. A. *J. Phys. Chem.* **1994**, *98*, 5441−5444. Botcher, T. R.; Wight, C. A. *J. Phys. Chem.* **1993**, *97*, 9149−9153.

(6) (a) Saxon, R. P.; Yoshimine, M. *J. Phys. Chem.* **1989**, *93*, 3130−3135. (b) Saxon, R. P.; Yoshimine, M. *Can. J. Chem.* **1992**, *70*, 572. (c) McKee, M. L. *J. Phys. Chem.* **1989**, *93*, 7365−7374.

(7) Wodtke, A. M.; Hintsa, E. J.; Lee, Y. T. *J. Phys. Chem.* **1986**, *90*, 3549−3558.

(8) The magnitude of the KIE for global decomposition of solid HMX is 2.0 at 552 K and that for liquid RDX is 1.6 at 505 K. (a) Trulove, P. C.; Chapman, R. D.; Shackelford, S. A. *Propellants, Explos., Pyrotech.* **1994**, *19*, 42−58, and references cited therein. (b) Shackelford, S. A. In *Chemistry and Physics of Energetic Materials*; Bulusu, S. N., Ed.; Kluwer: Dordrecht, The Netherlands, 1990; p 413−432.

(9) Shaw, R.; Walker, F. E. *J. Phys. Chem.* **1977**, *81*, 2572−2576.

(10) (a) Capellos, C.; Papagiannakopoulos, P.; Liang, Y.-L. *Chem. Phys. Lett.* **1989**, *164*, 533−538. (b) Zuckermann, H.; Greenblatt, G. D.; Haas, Y. *J. Phys. Chem.* **1987**, *91*, 5159.

(11) Spokes, G. N.; Benson, S. W. *J. Am. Chem. Soc.* **1967**, *89*, 6030.

(12) Frisch, M. J.; Trucks, G. W.; Schlegel, H. B.; Gill, P. M. W.; Johnson, B. G.; Robb, M. A.; Cheeseman, J. R.; Keith, T.; Petersson, G. A.; Montgomery, J. A.; Raghavachari, K.; Al-Laham, M. A.; Zakrzewski, V. G.; Ortiz, J. V.; Foresman, J. B.; Cioslowski, J.; Stefanov, B. B.; Nanayakkara, A.; Challacombe, M.; Peng, C. Y.; Ayala, P. Y.; Chen, W.; Wong, M. W.; Andres, J. L.; Replogle, E. S.; Gomperts, R.; Martin, R. L.; Fox, D. J.; Binkley, J. S.; Defrees, D. J.; Baker, J.; Stewart, J. P.; Head-Gordon, M.; Gonzalez, C.; Pople, J. A. *Gaussian 94*, Revision B.1; Gaussian, Inc.: Pittsburgh, PA, 1995.

(13) (a) Becke, A. D. *J. Chem. Phys.* **1993**, *98*, 5648. (b) Lee, C.; Yang, W.; Parr, R. G. *Phys. Rev.* **1988**, *B37*, 785. (c) Stephens, P. J.; Devlin, F. J.; Chabalowski, C. F.; Frisch, M. J. *J. Phys. Chem.* **1994**, *98*, 11623, and references cited therein.

(14) Frisch, M. J.; Frisch, A.; Foresman, J. B. *Gaussian 94 User's Reference*; Gaussian, Inc.: Pittsburgh, PA, 1994.

(15) (a) Hehre, W. J.; Radom, L.; Schleyer, P. v. R. *Ab Initio Molecular Orbital Theory*; Wiley-Interscience: New York, 1986. (b) The PMP2/6-31G* energies for DMNA, Me_2N, TS, and NO_2 are respectively −338.665 8926, −134.021 5927, −338.572 2034, and −204.564 1962 hartrees. The respective PMP2/6-31G* zero-point vibrational energies are 61.55, 50.11, 56.57, and 6.30 kcal/mol.

(16) (a) Wolfsberg, M. *Acc. Chem. Res.* **1972**, *5*, 225. (b) Bigeleisen, J.; Mayer, M. G. *J. Chem. Phys.* **1947**, *15*, 261. (c) Harris, N. J. *J. Phys. Chem.* **1995**, *99*, 14689−14699.

(17) (a) Bigeleisen, J. *J. Chem. Phys.* **1949**, *17*, 675−678. (b) Saunders, W. H., Jr. In *Investigation of Rates and Mechanisms of Reactions*, 4th ed.; Bernasconi, C. F., Ed.; Wiley: New York, 1986; Part 1.

(18) Bell, R. P. *Trans. Faraday Soc.* **1959**, *55*, 1.

(19) (a) Krebs, B.; Mandt, J.; Cobbledick, R. E.; Small, R. W. H. *Acta Crystallogr.* **1979**, *B35*, 402−404. (b) Stoelevik, R.; Rademacher, P. *Acta Chem. Scand.* **1969**, *23*, 672.

(20) For a detailed discussion of inversion barriers and resonance in nitramines see: Ritchie, J. P. *J. Am. Chem. Soc.* **1989**, *111*, 2517−2520.

(21) Melius, C. F. In *Chemistry and Physics of Energetic Materials*; Bulusu, S. N., Ed.; Kluwer: Dordrecht, The Netherlands, 1990; p 21−50.

(22) For G2 theory see: Curtiss, L. A.; Carpenter, J. E.; Raghavachari, K.; Pople, J. A. *J. Chem. Phys.* **1992**, *96*, 9030. Curtis, L. A.; Jones, C.; Trucks, G. W.; Raghavachari, K.; Pople, J. A. *J. Chem. Phys.* **1990**, *93*, 2537.

(23) Mowrey, R. C.; Page, M. *J. Chem. Phys.* **1990**, *93*, 1857−1864.

(24) Shiner, V. J., Jr.; Neumann, T. E. *Z. Naturforsch.* **1989**, *44A*, 337−354. See also: Hartshorn, S. R.; Shiner, V. J., Jr. *J. Am. Chem. Soc.* **1972**, *94*, 9002−9012.

(25) DeFrees, D. J.; Taagepera, M.; Levi, B. A.; Pollack, S. K.; Summerhays, K. D.; Taft, R. W.; Wolfsberg, M.; Hehre, W. J. *J. Am. Chem. Soc.* **1979**, *101*, 5532−5536. DeFrees, D. J.; Hassner, D. Z.; Hehre, W. J.; Peter, E. A.; Wolfsberg, M. *J. Am. Chem. Soc.* **1978**, *100*, 641. See also: Steigerwald, M. L.; Goddard, W. A., III; Evans, D. A. *J. Am. Chem. Soc.* **1979**, *101*, 1994−1997.

(26) (a) We use $\alpha = k_1/(k_1 + k_2)$ for the fraction of total reaction which goes by N−N cleavage, and $1 - \alpha = k_2/(k_1 + k_2)$ for the fraction which goes by HONO elimination. Note that $k_{obs}^H/k_{obs}^{D6} = (k_1^H + k_2^H)/(k_1^{D6} + k_2^{D6})$. Then

$$\alpha^H = \alpha^{D6}[(k_1^H/k_1^{D6})/(k_{obs}^H/k_{obs}^{D6})] \quad (1)$$

$$1 - \alpha^H = (1 - \alpha^{D6})[(k_2^H/k_2^{D6})/(k_{obs}^H/k_{obs}^{D6})] \quad (2)$$

Adding eqs 1 and 2 and solving for α^{D6} gives $\alpha^{D6} = (k_2^H/k_2^{D6} - k_{obs}^H/k_{obs}^{D6})/(k_2^H/k_2^{D6} - k_1^H/k_1^{D6}) = (4.21 - 1.57)/(4.21 - 1.40) = 0.939$. We can now compute α^H, by substituting the known value of α^{D6} into eq 1: $\alpha^H = 0.939(1.40/1.57) = 0.838$. Thus $\alpha^H = 0.838$ and $\alpha^{D6} = 0.939$. The branching ratios for H and D are then given by $k_1^H/k_2^H = \alpha^H/(1 - \alpha^H)$ and $k_1^{D6}/k_2^{D6} = \alpha^{D6}/(1 - \alpha^{D6})$. (b) For example, if the error range in the observed KIE is 0.15, then the value for α^{D6} could be as large as 0.99 or as small as 0.89. Of course, error in the theoretical isotope effects must also be considered.

(27) (a) Behrens, R., Jr.; Bulusu, S. *J. Phys. Chem.* **1992**, *96*, 8891−8897; 8877−8891. (b) Behrens, R., Jr.; Bulusu, S. *J. Phys. Chem.* **1991**, *95*, 5838−5845. (c) Behrens, R., Jr. *J. Phys. Chem.* **1990**, *94*, 6706−6718. (d) Behrens, R., Jr. In *Chemistry and Physics of Energetic Materials*; Bulusu, S. N., Ed.; Kluwer: Dordrecht, The Netherlands, 1990; pp 347−368. (e) Brill, T. B. *J. Propuls. Power* **1995**, *11*, 740−751.